Single-Molecule Resonant Tunneling Diode

ARTICLE *in* THE JOURNAL OF PHYSICAL CHEMISTRY C · FEBRUARY 2015

Impact Factor: 4.77 · DOI: 10.1021/jp512803s

6 AUTHORS, INCLUDING:

Mickael Lucien Perrin

Delft University of Technology

13 PUBLICATIONS **97** CITATIONS

SEE PROFILE

Elena Galán

Delft University of Technology

12 PUBLICATIONS **92** CITATIONS

SEE PROFILE

Rienk Eelkema

Delft University of Technology

51 PUBLICATIONS **1,408** CITATIONS

SEE PROFILE

F.C. Grozema

Delft University of Technology

129 PUBLICATIONS **3,724** CITATIONS

SEE PROFILE

THE JOURNAL OF PHYSICAL CHEMISTRY C

Article

pubs.acs.org/JPCC

Single-Molecule Resonant Tunneling Diode

Mickael L. Perrin,[†] Elena Galan,[‡] Rienk Eelkema,[‡] Ferdinand Grozema,[‡] Joseph M. Thijssen,[†] and Herre S. J. van der Zant*,[†]

[†]Kavli Institute of Nanoscience, Delft University of Technology, Lorentzweg 1, 2628 CJ Delft, The Netherlands

[‡]Department of Chemical Engineering, Delft University of Technology, Julianalaan 136, 2628 BL Delft, The Netherlands

Supporting Information

ABSTRACT: Rectification has been at the foundation of molecular electronics. Most single-molecule diodes realized experimentally so far are based on asymmetries in the coupling with the electrodes or using the donor−acceptor principle. In general, however, their rectification ratios are usually small (<10). Here, we propose a single-molecule diode based on an orbital resonance while using the highest occupied molecular orbital (HOMO) and HOMO−1 as transport channels. Our proposed diode design is based on an asymmetric two-site model and analyzed with DFT + NEGF calculations. We find high rectification ratios, even in the case of symmetric coupling to the electrodes. In addition, we show that diode parameters such as the operating voltage and rectification ratio can be tuned by chemical design.

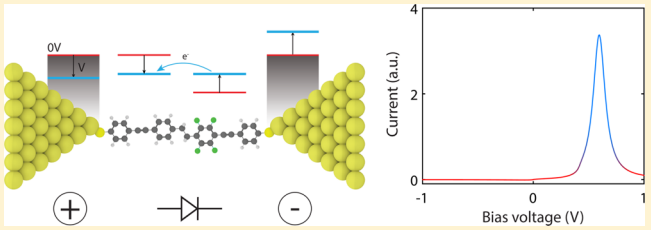

INTRODUCTION

The molecular diode is the seminal proposal which started the field of single-molecule electronics[1] with the original design inspired by semiconducting p-n junctions. As one side of the molecule was electron rich and the other electron poor, one current direction was favored above the other. Since that proposal, other theoretical predictions and models have been proposed based on other mechanisms such as asymmetric tunneling barriers[2,3] or asymmetric charging.[4] From an experimental point of view, rectification ratios (current ratio between the forward and reverse bias) as high as 100 have been reported in measurements on self-assembled monolayers.[5] On the single-molecule scale, however, this figure of merit has not exceeded 10, whether rectification was based on asymmetries in the coupling to the electrodes,[6,7] quantum interference,[8] or the donor−acceptor principle.[9−12]

In this paper, we present a design for single-molecule diodes based on orbital resonances and demonstrate that this mechanism leads to large rectification ratios. Using density functional theory (DFT) and the non-equilibrium Green's function (NEGF) formalism, we investigate how different electron-withdrawing and -donating substituents alter the current voltage characteristics. Finally, we demonstrate that for an appropriate choice of substituents unprecedented rectification ratios above 1000 may be achieved.

The diode mechanism we propose is based on intramolecular coherent resonant transport, in contrast to the Aviram−Ratner rectifier,[1] where charge transport is vibrationally assisted. We use a molecule that consists of two conjugated parts that are coupled together through a non-conjugated linker. Due to the non-conjugated linker, the molecule can be seen as two weakly coupled sites in series. In such a system, resonant transport occurs only when the energy of the two sites is equal. A similar concept has been used recently to generate negative differential conductance (NDC) in a single-molecule junction.[13] The origin of the NDC is explained as follows: at zero bias, the two sites were at equal energy and resonant charge transport occurred. By applying a bias voltage, the energy of the sites was shifted apart and the resonance condition was lifted, thereby suppressing transport.

When an asymmetry is introduced in such a molecular structure, for instance, by adding electron-withdrawing or -donating groups on one side, the energy of the sites becomes different and the resonance condition between the two halves of the molecule can then only be reached by shifting the energy of the sites with respect to each other. This shift can be achieved, for instance, by using Stark shifts induced by a bias voltage. However, as the resonant condition can only be reached for a particular bias polarity, the antisymmetry of the current−voltage characteristics is lifted and the molecule behaves as a diode.

The diode mechanism is schematically depicted in Figure 1. At zero bias (see Figure 1a), the left site is at energy ε_1 while the right one is at ε_2. As the zero-bias energy splitting $(\varepsilon_1 - \varepsilon_2)$ is nonzero, this leads to a low zero-bias conductance. In the model, $\Gamma_{L,R}$ accounts for the electronic coupling of the left (L) and right (R) site to the corresponding electrode. Upon application of a positive bias, the two sites are pulled toward each other as a result of a bias-induced Stark Shift until they reach a resonant condition at a bias voltage of $V_p = (\varepsilon_1 - \varepsilon_2)/\alpha$,

Received: December 23, 2014
Revised: February 12, 2015
Published: February 12, 2015

DOI: 10.1021/jp512803s
J. Phys. Chem. C 2015, 119, 5697−5702

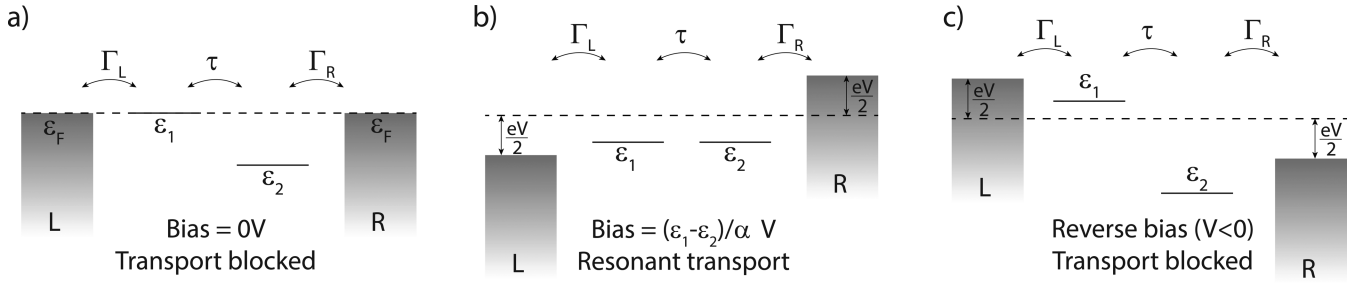

Figure 1. Diode mechanism. Schematics illustrating charge transport in an asymmetric molecule in the case of (a) zero bias, (b) forward bias on resonance, and (c) reverse bias. $\varepsilon_{1,2}$ are the on-site energies, τ the intersite coupling, and α the fraction of the voltage that drops inside the molecule.

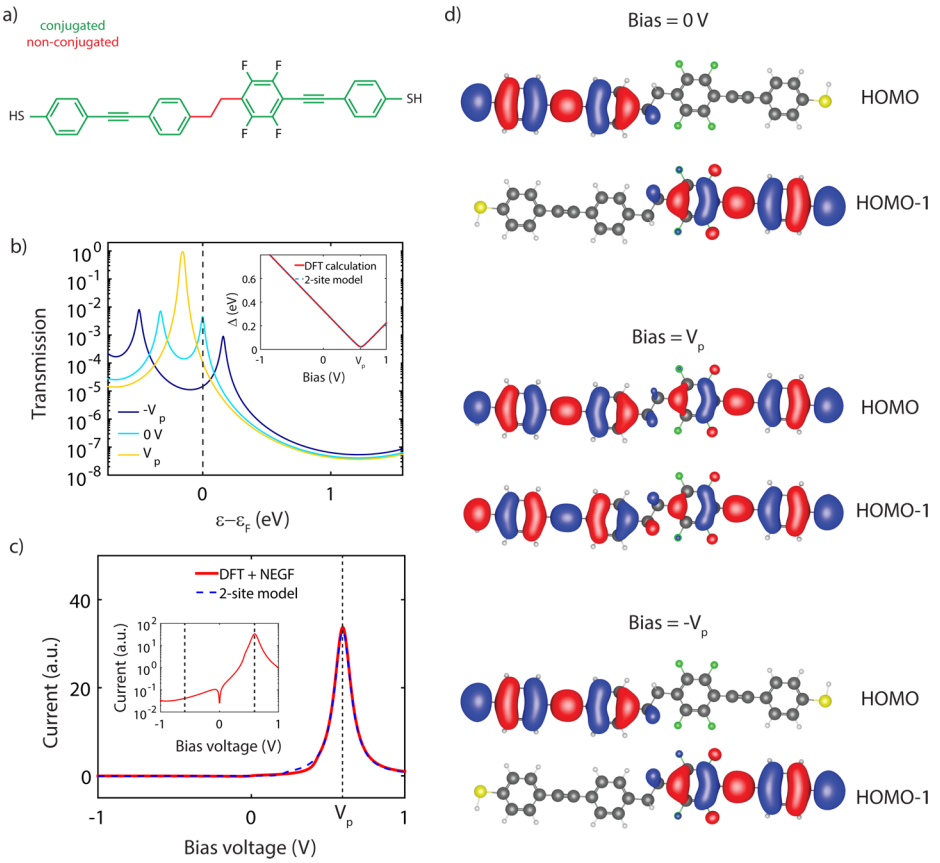

Figure 2. DFT + NEGF calculation on proposed diode molecule. (a) Chemical structure of 1,2-bis(4-(phenylethynyl)phenyl)ethane: (green) conjugated parts of the molecule, (red) non-conjugated ones. (b) Transmission for various bias voltages. Dashed line indicates the assumed position of the Fermi energy. (Inset) Energy difference between the HOMO and the HOMO−1 (Δ) as a function of bias voltage. Fit parameters are α = 0.55, τ = 10.9 meV, and $\varepsilon_1 - \varepsilon_2$ = 329 meV. (c) *IV* characteristic calculated using DFT + NEGF (solid red, Γ = 100 meV) and using the two-site model (dashed blue, Γ = 29.0 meV). (d) HOMO and HOMO−1 in the case of a bias voltage of (top) 0 V, (middle) V_p, and (bottom) $-V_p$.

where α describes the fraction of the voltage that drops inside the molecule. It is important to realize that the voltage drop inside the molecule is essential for the rectification mechanism. Upon approaching the resonance condition, the conductance drastically increases (see Figure 1b). For larger bias, the sites are pulled off-resonance again and the conductance decreases. Therefore, a peak in the current at a bias voltage of V_p is expected. For negative bias, the sites are increasingly pulled away from each other and the conductance remains low for all voltages (see Figure 1c).

The transport properties of such an asymmetric two-site system can be described using the following Hamiltonian

$$\mathbf{H} = \begin{pmatrix} \varepsilon_1 + \frac{1}{2}\alpha eV & -\tau \\ -\tau & \varepsilon_2 - \frac{1}{2}\alpha eV \end{pmatrix} \quad (1)$$

The eigenstates of this Hamiltonian correspond to the bonding (π) and antibonding (π^*) orbitals where their energy splitting Δ in the presence of a bias voltage is given by

$$\Delta = \sqrt{(\alpha eV)^2 + 2\alpha eV(\varepsilon_1 - \varepsilon_2) + (\varepsilon_1 - \varepsilon_2)^2 + (2\tau)^2} \quad (2)$$

We now symmetrically couple the left and right sites to the corresponding leads in the wide-band limit[14,15]

DOI: 10.1021/jp512803s
J. Phys. Chem. C 2015, 119, 5697−5702

$$\Gamma_L = \begin{pmatrix} \Gamma & 0 \\ 0 & 0 \end{pmatrix}, \quad \Gamma_R = \begin{pmatrix} 0 & 0 \\ 0 & \Gamma \end{pmatrix} \tag{3}$$

The transmission is given by[14−16]

$$\mathcal{T}(\varepsilon) = Tr\{\Gamma_L \mathbf{G}^r(\varepsilon)\Gamma_R \mathbf{G}^a(\varepsilon)\} \tag{4}$$

where $\mathbf{G}^r(\varepsilon)$ and $\mathbf{G}^a(\varepsilon)$ are the retarded and advanced Green's functions, respectively. The former is given by

$$\mathbf{G}^r(\varepsilon) = \left(\varepsilon \mathbf{1} - \mathbf{H} + \frac{i}{2}(\Gamma_L + \Gamma_R)\right)^{-1} \tag{5}$$

while $\mathbf{G}^a(\varepsilon) = \mathbf{G}^r(\varepsilon)$. The current can be calculated via[14−16]

$$I = \frac{2e}{\hbar} \int \frac{d\varepsilon}{2\pi} (f_L(\varepsilon) - f_R(\varepsilon))\mathcal{T}(\varepsilon) \tag{6}$$

where $f_L(\varepsilon)$ and $f_R(\varepsilon)$ are the Fermi functions of the left and right lead, respectively.

As noted above, charge transport through a molecule consisting of two conjugated parts that are weakly coupled should follow the behavior of the two-site model described above (see discussion, Figure 1). The weak coupling between sites can, for example, be realized by introducing either a twisted biphenyl moiety[17,18] or a saturated (Csp^3) carbon chain.[1] The former method has the drawback that the degree of conjugation (and thus the conductance) throughout the molecule strongly depends on the torsion angle between the phenyl rings. As a result, the intersite coupling τ may vary as well, rendering the diode performance very sensitive to the molecular conformation. When using the latter method, one has to keep in mind that the more saturated carbon atoms are connected in series to form the non-conjugated segment, the lower τ becomes. Although this increases the rectification ratio (see section II of the Supporting Information), the decrease in τ is accompanied by a decrease in the maximum elastic current flowing through the molecule down to a negligible value, where only inelastic contributions to the current remain.[1] Another way to create a weak coupling is to use cross-conjugation.[19,20]

Next to the formation of two weakly coupled halves, the molecule should fulfill additional requirements. We now list some of them. First, transport through the molecule should be dominated by the HOMO and HOMO−1, as their splitting can be tuned more easily compared to, for instance, the HOMO and LUMO. This can be achieved by using a symmetric backbone in combination with a weak intersite coupling. This promotes the formation of bonding/antibonding orbitals for the HOMO−1 and HOMO, which are closely located in energy and can be used for transport.

Second, one should keep in mind that for organic, conjugated molecules, in general, the larger the molecule becomes the closer the energies levels are with respect to each other. As soon as the HOMO−2 and lower lying orbitals are located so close to the HOMO and HOMO−1 that they also significantly contribute to transport, a parallel transport channel opens up and the two-site approximation ceases to hold.

Third, a proper choice for the anchoring groups has to be made. Next to determining the electronic coupling and the level alignment,[21] they also influence how the voltage drops inside the molecule, see section III of the Supporting Information. In addition, the anchoring groups also modify the wave function of the HOMO and HOMO−1 and hence the intersite coupling τ. Fourth, electron-withdrawing/donating groups need to be added to the molecule in an asymmetric way, such that one of the halves is lowered or shifted up in energy. Finally, as we will show in the following, the HOMO should be located as close as possible to the Fermi energy for the highest rectification ratio.

Taking all the above-mentioned considerations into account, we choose molecules which are comparable in chemical structure to the one used by Perrin et al.[13] and with comparable values for α and τ. To break the conjugation, we use diphenylethane (see Figure 2a), to which phenylethynyl spacers are connected.[22] Thiols are used as the anchoring group, as they favor hole transport.[23] For the symmetric, unsubstituted molecule we find that transport can indeed be modeled as two sites in series and that a pronounced NDC feature arises, see section I of the Supporting Information. The asymmetry in the molecule is initially introduced by adding four fluorine atoms to the right half of the molecule.

THEORETICAL METHODS

To investigate the electronic structure of the molecule, density functional theory (DFT) calculations were performed using the Amsterdam Density Functional (ADF) package with the GGA PBE exchange-correlation functional and the triple-ζ plus polarization (TZP) basis set.[24,25] Transmissions were calculated from DFT within the nonequilibrium Green's function (NEGF) framework by coupling the p_z orbitals of the sulfur atoms to wide-band electrodes[13,26] with a coupling strength of 100 meV. A bias voltage was applied to the molecule by introducing a uniform electric field along the axis connecting the sulfur atoms.

RESULTS AND DISCUSSION

In Figure 2b the transmission through the molecule is plotted. For now, we assume that at zero bias the HOMO is on resonance with the Fermi energy E_F. The HOMO−1 is in this case located 0.33 eV below it. The amplitudes of the transmission peaks corresponding to the HOMO and HOMO−1 resonances are less than 1×10^{-2} G_0. The HOMO−2 (located more than 1 eV away) and the lowest unoccupied molecular orbital (LUMO, 2.3 eV above E_F) are too far from the Fermi energy and do not contribute to transport. The upper panel of Figure 2d shows the HOMO and HOMO−1 at zero bias, each of which is localized on one-half of the molecule. Due to their localized character, their transmission remains low, which is reflected in the current−voltage characteristic (IV) plotted in Figure 2c. Upon application of a bias, the HOMO and HOMO−1 shift due to the Stark effect. The inset of Figure 2b displays the energy splitting of the HOMO and HOMO−1, denoted as Δ, accompanied by a fit to eq 2, from which the two-site model parameters α, τ, and $\varepsilon_1 - \varepsilon_2$ are obtained. For an increasing positive bias, Δ initially decreases linearly until it reaches a minimum at V_p, which is located at 0.59 V. At V_p, the HOMO and HOMO−1 are delocalized (see the middle panel of Figure 2d) and fully extended across the entire molecule. This delocalization causes the amplitude of the resonances to increase to unity. The transmission shows a single resonance, as the HOMO and HOMO−1 are nearly degenerate, with $\Delta \ll \Gamma_{L,R}$. The current also increases and shows a maximum at V_p. When increasing the bias beyond V_p, Δ increases and the amplitude of the transmission decreases, resulting in a decrease of the current. For negative bias, the orbitals remain localized and Δ increases linearly with bias voltage. As the amplitude of

DOI: 10.1021/jp512803s
J. Phys. Chem. C 2015, 119, 5697−5702

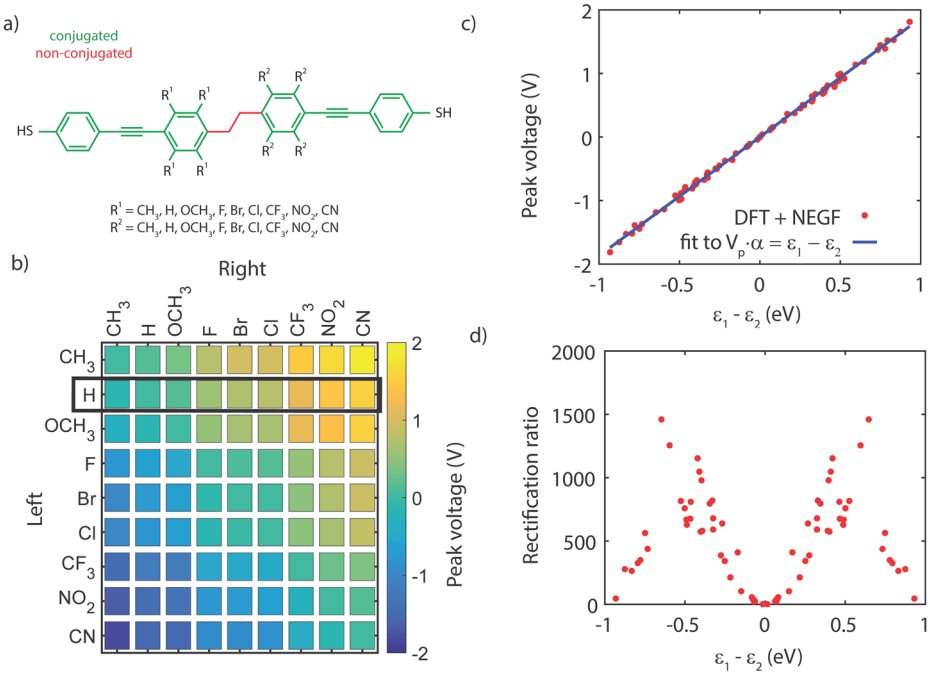

Figure 3. DFT + NEGF calculation upon variation of the functional groups. (a) Chemical structure of all of the molecules calculated: (green) conjugated halves of the molecule, (red) non-conjugated segment. (b) Peak voltage of all 45 combinations of molecules. (c) Peak voltage as a function of level splitting $\varepsilon_1 - \varepsilon_2$ (red dots). Blue line is a fit to extract the value of α, which is 0.53. (d) Rectification ratio as a function of level splitting $\varepsilon_1 - \varepsilon_2$.

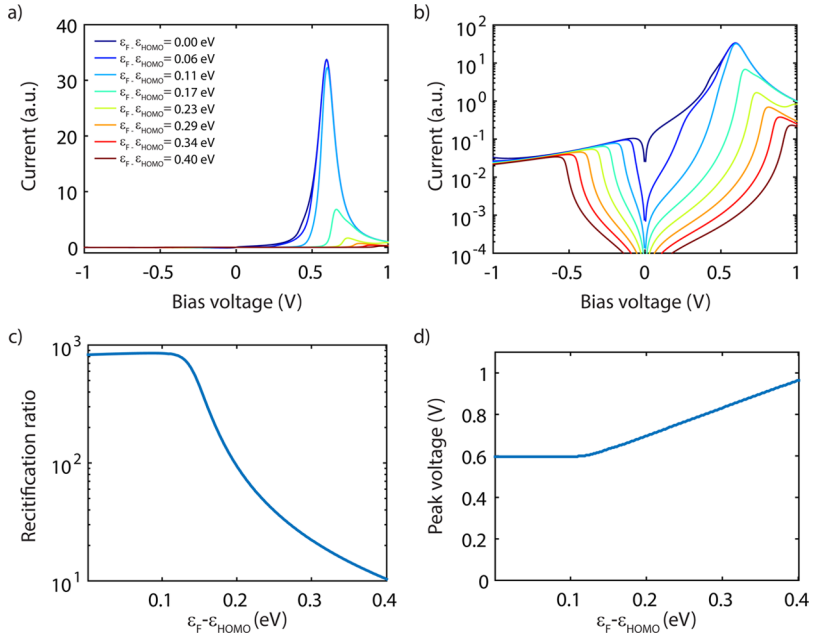

Figure 4. Dependence of diode characteristics on level alignment. *IV* characteristics calculated using DFT + NEGF for various level alignment shown on a (a) linear scale and (b) logarithmic scale. (c) Rectification ratio and (d) peak voltage dependence on the level alignment.

the transmission resonances stays below 1×10^{-2} G_0, the current remains low.

The DFT + NEGF calculation shows that this molecule behaves as a diode. Important characteristics of this rectifier are the peak voltage (V_p) and the current ratio between forward and reverse bias. As the definition for the rectification ratio (RR) we use the ratio between the current at V_p and $-V_p$. For the molecule of Figure 1a we obtain RR = 820. Using the values for α, τ, and $\varepsilon_1 - \varepsilon_2$ obtained in the inset of Figure 2b, we can calculate the current−voltage characteristic predicted by the two-site model using expression 6, as illustrated by the blue dashed line. The two-site model reproduces the DFT + NEGF calculation well, indicating the two-site model can be used to describe the molecule.

To investigate the role of the side groups on RR and V_p, we calculated the electronic structure and *IV* characteristics for nine different functional groups (CH_3, H, OCH_3, Br, Cl, CF_3, NO_2, CN). We varied the side groups of both halves of the

DOI: 10.1021/jp512803s
J. Phys. Chem. C 2015, 119, 5697−5702

molecule, resulting in 45 different molecules (see Figure 3a). For each molecule we extracted RR and V_p, assuming the HOMO to be on resonance with the Fermi energy at $V = 0$. Figure 3b shows a matrix for the 45 different molecules, with the color scale representing V_p. The side groups have been sorted as a function of V_p with on the left side hydrogen atoms (R^1 = H), see the highlighted row. On the diagonal, the molecules are symmetric and NDC is observed. As one moves away from the diagonal, the molecule behaves as a rectifier and the absolute value of the peak voltage increases. The matrix is antisymmetric, as swapping the left and right side groups leads to the same peak at opposite voltage. In Figure 3c, V_p is plotted as a function of the energy splitting. The peak voltage V_p scales linearly with $\varepsilon_1 - \varepsilon_2$. By linearly fitting the data, we obtain a value for α of 0.53. The fact that α is very similar for all combinations of side groups indicates that α is related to the backbone and/or the anchoring groups and not to the side groups. In addition, the total level splitting obtained when combining two side groups is close to the sum of the energy splitting of the individual side groups, i.e., one can estimate within 50 meV (see section V of the Supporting Information for more details) the splitting of a combination of side groups by adding the level splittings obtained from the highlighted row. The fact that one can simply add the individual level splitting is due to the weak coupling between the two halves of the molecule. In section VI of the Supporting Information we show that, in fact, the level splitting scales linearly with the Hammett constant.

In Figure 3d, RR is plotted as a function of $\varepsilon_1 - \varepsilon_2$. RR is low for small $\varepsilon_1 - \varepsilon_2$ and increases to a maximum of about 1500 at an energy splitting of around 0.6 eV. For larger splitting, RR decreases again. This trend can be understood as follows. For low-energy splitting, the tail of the transmissions of the two sites feel each other, leading to a relatively high reverse bias current and hence a low RR. Increasing $\varepsilon_1 - \varepsilon_2$ up to 0.6 eV reduces this parasitic current in reverse bias mode and hence improves RR. For $\varepsilon_1 - \varepsilon_2$ larger than 0.6 eV, however, additional orbitals start to come into play, increasing the reverse current and reducing RR.

In the previous analysis, we took the HOMO to be on resonance with the Fermi energy. From a theoretical point of view, predicting the exact location of the Fermi energy is very difficult. In Figure 4 we show the diode characteristics for increasing level misalignment between the HOMO and ε_F. Figure 4a and 4b present the *IV* characteristics for various level alignments. In Figure 4c and 4d RR and the peak voltage are given. Both remain fairly constant within 150 meV at a value of about 800 and 0.6 V, respectively. For misalignments beyond this bias voltage, RR quickly decays and reaches the value 10 at around 400 meV. The peak voltage, on the other hand, nearly linearly increases up to 0.95 V. For conjugated, thiol-anchored molecular wires, the location of the HOMO is reported to be within 0.5 eV below the Fermi energy.[27] Due to sample-to-sample variation of the level alignment, RR can therefore vary from below 10 to above 100. To realize high rectification ratios in experiments, the use of an electrostatic[28−31] or chemical gate[32,33] to control the position of the occupied levels with respect to the Fermi energy may be necessary. Next to variations in the level alignment, different molecular geometries may occur during experiments, leading to variations in τ and Γ and hence variations in RR.

We would like to emphasize that the fact that the peak voltage can be tuned from milliVolts to Volts is due to the symmetry of the backbone of the unsubstituted molecule. This symmetry is crucial as it yields a HOMO−1 and HOMO that are nearly degenerate and with bonding/antibonding character. The splitting between the two orbitals can then easily be changed by introducing electron-donating/withdrawing groups and allows for fine tuning of the diode properties.

In the DFT + NEGF calculations, the charge is injected into the p_z orbitals of the sulfur atoms. Although the π orbitals constitute the largest contribution to the current through the molecule,[26] this approach underestimates the contribution of the σ orbitals and, hence, slightly overestimates the RR.

In our analysis, we used nine side groups. In fact, many more could be used, as long as they have electron-withdrawing/donating properties. However, one has to make sure that the HOMO and HOMO−1 of the resulting molecule are the ones originating from the two-site structure and yielding rectification. Some substituents, such as OH, COOH, NH_2, and $C(CH_3)_3$, have a HOMO and/or HOMO−1 which is located on the side groups only and does not contribute to transport. Such substituents are not suited, as one has first to depopulate the localized HOMO and/or the HOMO−1 in order to align the orbitals yielding the rectification with the Fermi energy.

Finally, we note that RR can be improved further by tweaking Γ and τ. As a rule of thumb, the lower Γ and τ the higher RR becomes (see sections II and IV of the Supporting Information) but also the lower the maximum current. RR can be further improved using molecules with the orbitals further apart, thereby reducing the current in reverse bias mode. Another way to suppress the current in reverse bias mode may be to use destructive quantum interference.[34] Other approaches, such as asymmetries in the anchoring groups, could also be envisioned.

CONCLUSIONS

We discussed the design of a single-molecule resonant tunneling diode of which the operation is based on an intuitive two-site model. The proposed molecule consists of two weakly coupled molecular halves and allows one to generate high rectification ratios. Using DFT + NEGF calculations, we explore the different model parameters and relate them to the chemical structure of the molecule. We find that, due to the weak coupling between the two halves of the molecule, the peak voltage and rectification ratio can be tuned by chemically modifying the molecule. Our findings provide design guidelines for highly efficient single-molecule rectifiers.

ASSOCIATED CONTENT

Supporting Information

DFT + NEGF calculations for the unsubstituted molecule, for varying linker length, for a different anchoring group, for the variation of the electronic coupling strength, for the error estimation of the level splitting $\varepsilon_1 - \varepsilon_2$, and for the relation between the level splitting $\varepsilon_1 - \varepsilon_2$ and the Hammett constant. This material is available free of charge via the Internet at http://pubs.acs.org.

AUTHOR INFORMATION

Corresponding Author

*E-mail: h.s.j.vanderzant@tudelft.nl.

Notes

The authors declare no competing financial interest.

DOI: 10.1021/jp512803s
J. Phys. Chem. C 2015, 119, 5697−5702

■ ACKNOWLEDGMENTS

This research was carried out with financial support from the Dutch Foundation for Fundamental Research on Matter (FOM), the Dutch Organisation for Scientific Research (NWO), the Ministry of Education, Culture and Science (OCW), the FP7-framework program ELFOS, ERC Grant no. 240299, and by an ERC advanced grant (Mols@Mols). We thank Dr. Johannes S. Seldenthuis for help with the DFT + NEGF calculations.

■ REFERENCES

(1) Aviram, A.; Ratner, M. A. Molecular Rectifiers. *Chem. Phys. Lett.* **1974**, *29*, 277−283.
(2) Kornilovitch, P. E.; Bratkovsky, A. M.; Stanley Williams, R. Current Rectification by Molecules with Asymmetric Tunneling Barriers. *Phys. Rev. B* **2002**, *66*, 165436−165446.
(3) Taylor, J.; Brandbyge, M.; Stokbro, K. Theory of Rectification in Tour Wires: The Role of Electrode Coupling. *Phys. Rev. Lett.* **2002**, *89*, 138301−138304.
(4) Paulsson, M.; Zahid, F.; Datta, S. *Handbook of Nanoscience Engineering, and Technology*; CRC Press: Boca Raton, FL, 2003.
(5) Nijhuis, C. A.; Reus, W. F.; Whitesides, G. M. Molecular Rectification in Metal-SAM-Metal Oxide-Metal Junctions. *J. Am. Chem. Soc.* **2009**, *131*, 17814−17827.
(6) Batra, A.; Darancet, P.; Chen, Q.; Meisner, J. S.; Widawsky, J. R.; Neaton, J. B.; Nuckolls, C.; Venkataraman, L. Tuning Rectification in Single-Molecular Diodes. *Nano Lett.* **2013**, *13*, 6233−6237.
(7) Kim, T.; Liu, Z. F.; Lee, C.; Neaton, J. B.; Venkataraman, L. Charge Transport and Rectification in Molecular Junctions Formed with Carbon-Based Electrodes. *Proc. Natl. Acad. Sci. U.S.A.* **2014**, *111*, 10928−10932.
(8) Batra, A.; Meisner, J. S.; Darancet, P.; Chen, Q.; Steigerwald, M. L.; Nuckolls, C.; Venkataraman, L. Molecular Diodes Enabled by Quantum Interference. *Faraday Discuss.* **2014**, *174*, 79−89.
(9) Elbing, M.; Ochs, R.; Koentopp, M.; Fischer, M.; von Hanisch, C.; Weigend, F.; Evers, F.; Weber, H. B.; Mayor, M. A Single-Molecule Diode. *Proc. Natl. Acad. Sci. U.S.A.* **2005**, *102*, 8815−8820.
(10) Diez-Perez, I.; Hihath, J.; Lee, Y.; Yu, L.; Adamska, L.; Kozhushner, M. A.; Oleynik, I. I.; Tao, N. J. Rectification and Stability of a Single-Molecular Diode with Controlled Orientation. *Nat. Chem.* **2009**, *1*, 635−641.
(11) Hihath, J.; Bruot, C.; Nakamura, H.; Asai, Y.; Diez-Perez, I.; Lee, Y.; Yu, L.; Tao, N. J. Inelastic Transport and Low-Bias Rectification in a Single-Molecule Diode. *ACS Nano* **2011**, *5*, 8331−8339.
(12) Lörtscher, E.; Gotsmann, B.; Lee, Y.; Yu, L.; Rettner, C.; Riel, H. Transport Properties of a Single-Molecule Diode. *ACS Nano* **2012**, *6*, 4931−4939.
(13) Perrin, M. L.; Frisenda, R.; Koole, M.; Seldenthuis, J. S.; Celis Gil, J.; Valkenier, H.; Hummelen, J. C.; Renaud, N.; Grozema, F. C.; Thijssen, J. M.; et al. Large Negative Differential Conductance in Single-Molecule Break Junctions. *Nat. Nanotechnol.* **2014**, *9*, 830−834.
(14) Jauho, A.-P.; Wingreen, N. S.; Meir, Y. Time-Dependent Transport in Interacting and Noninteracting Resonant-Tunneling Systems. *Phys. Rev. B* **1994**, *50*, 5528−5544.
(15) Haug, H.; Jauho, A.-P. *Quantum Kinetics in Transport and Optics of Semiconductors*; Springer: Berlin, Heidelberg, 1997.
(16) Meir, Y.; Wingreen, N. S. Landauer Formula for the Current Through an Interacting Electron Region. *Phys. Rev. Lett.* **1992**, *68*, 2512−2515.
(17) Venkataraman, L.; Klare, J. E.; Nuckolls, C.; Hybertsen, M. S.; Steigerwald, M. L. Dependence of Single-Molecule Junction Conductance On Molecular Conformation. *Nature* **2006**, *442*, 904−907.
(18) Mishchenko, A.; Vonlanthen, D.; Meded, V.; Bürkle, M.; Li, C.; Pobelov, I.; Bagrets, A.; Viljas, J. K.; Pauly, F.; Evers, F.; et al. Influence of Conformation On Conductance of Biphenyl-Dithiol Single-Molecule Contacts. *Nano Lett.* **2010**, *10*, 156−163.
(19) Hong, W.; Valkenier, H.; Meszaros, G.; Manrique, D. Z.; Mishchenko, A.; Putz, A.; Moreno-García, P.; Lambert, C. J.; Hummelen, J. C.; Wandlowski, T. An MCBJ Case Study: The Influence of π-Conjugation On the Single-Molecule Conductance at a Solid/Liquid Interface. *Beilstein J. Nanotechnol.* **2011**, *2*, 699−713.
(20) Arroyo, C. R.; Tarkuc, S.; Frisenda, R.; Seldenthuis, J. S.; Woerde, C. H. M.; Eelkema, R.; Grozema, F. C.; Zant, H. S. J. Signatures of Quantum Interference Effects On Charge Transport Through a Single Benzene Ring. *Angew. Chem., Int. Ed.* **2013**, *52*, 3152−3155.
(21) Kaliginedi, V.; Rudnev, A. V.; Moreno-García, P.; Baghernejad, M.; Huang, C.; Hong, W.; Wandlowski, T. Promising Anchoring Groups for Single-Molecule Conductance Measurements. *Phys. Chem. Chem. Phys.* **2014**, *16*, 23529−23539.
(22) Stokbro, K.; Taylor, J.; Brandbyge, M. Do Aviram-Ratner Diodes Rectify? *J. Am. Chem. Soc.* **2003**, *125*, 3674−3675.
(23) Aradhya, S. V.; Venkataraman, L. Single-Molecule Junctions Beyond Electronic Transport. *Nat. Nanotechnol.* **2013**, *8*, 399−410.
(24) te Velde, G.; Bickelhaupt, F. M.; Gisbergen, S. J. A.; Fonseca Guerra, C.; Baerends, E. J.; Snijders, J. G.; Ziegler, T. Chemistry with ADF. *J. Comput. Chem.* **2001**, *22*, 931−967.
(25) Fonseca Guerra, C.; Snijders, J. G.; te Velde, G.; Baerends, E. J. Towards an Order-*N* DFT Method. *Theor. Chem. Acc.* **1998**, *99*, 391−403.
(26) Verzijl, C. J. O.; Seldenthuis, J. S.; Thijssen, J. M. Applicability of the Wide-Band Limit in DFT-Based Molecular Transport Calculations. *J. Chem. Phys.* **2013**, *138*, 094102−094111.
(27) Frisenda, R.; Perrin, M. L.; Valkenier, H.; Hummelen, J. C.; van der Zant, H. S. J. Statistical Analysis of Single-Molecule Breaking Traces. *Phys. Status Solidi B* **2013**, *250*, 2431−2436.
(28) Park, H.; Park, J.; Lim, A. K. L.; Anderson, E. H.; Alivisatos, A. P.; McEuen, P. L. Nanomechanical Oscillations in a Single-C_{60} Transistor. *Nature* **2000**, *407*, 57−60.
(29) Park, J.; Pasupathy, A. N.; Goldsmith, J. I.; Chang, C.; Yaish, Y.; Petta, J. R.; Rinkoski, M.; Sethna, J. P.; Abruna, H. D.; McEuen, P. L.; et al. Coulomb Blockade and the Kondo Effect in Single-Atom Transistors. *Nature* **2002**, *417*, 722−725.
(30) Kubatkin, S.; Danilov, D.; Hjort, M.; Cornil, J.; Bredas, J.- L.; Stuhr-Hansen, N.; Hedegard, P.; Bjornholm, T. Single-Electron Transistor of a Single Organic Molecule with Access to Several Redox States. *Nature* **2003**, *425*, 698−701.
(31) Perrin, M. L.; Verzijl, C. J. O.; Martin, C. A.; Shaikh, A. J.; Eelkema, R.; van Esch, J.; van Ruitenbeek, J. M.; Thijssen, J. M.; van der Zant, H. S. J.; Dulić, D. Large Tunable Image-Charge Effects in Single-Molecule Junctions. *Nat. Nanotechnol.* **2013**, *8*, 282−287.
(32) Capozzi, B.; Chen, Q.; Darancet, P.; Kotiuga, M.; Buzzeo, M.; Neaton, J. B.; Nuckolls, C.; Venkataraman, L. Tunable Charge Transport in Single-Molecule Junctions via Electrolytic Gating. *Nano Lett.* **2014**, *14*, 1400−1404.
(33) Baghernejad, M.; Manrique, D. Z.; Li, C.; Pope, T.; Zhumaev, U.; Pobelov, I.; Moreno-García, P.; Kaliginedi, V.; Huang, C.; Hong, W.; et al. Highly-Effective Gating of Single-Molecule Junctions: an Electrochemical Approach. *Chem. Commun.* **2014**, *50*, 15975−15978.
(34) Guedon, C. M.; Valkenier, H.; Markussen, T.; Thygesen, K. S.; Hummelen, J. C.; van der Molen, S. J. Observation of Quantum Interference in Molecular Charge Transport. *Nat. Nanotechnol.* **2012**, *7*, 304−308.

DOI: 10.1021/jp512803s
J. Phys. Chem. C 2015, 119, 5697−5702